AIAA JOURNAL
Vol. 40, No. 7, July 2002

Flexural Failure Behavior of Laminated Composites Reinforced with Braided Fabrics

Zheng-Ming Huang*
Tongji University, 200092 Shanghai, People's Republic of China
and
K. Fujihara† and S. Ramakrishna‡
National University of Singapore, Singapore 119260, Republic of Singapore

The failure behavior and ultimate strength of laminated textile composites subjected to bending is analyzed. Each ply in the laminate is a braided fabric reinforced lamina, with a different braiding angle if necessary. The overall load shared by the lamina in the laminate is determined by means of the classical lamination theory. After discretizing the lamina into small elements, the internal stresses generated in the constituent fiber and matrix materials of the lamina are calculated based on a general micromechanics model, the bridging model. A stress failure criterion is applied to check the lamina failure status, by comparing the internal stresses with their critical values. Unlike an in-plane load situation where the ultimate failure of the laminate corresponds to its last-ply failure, the ultimate bending strength of the laminate generally occurs before its last-ply failure. Thus, the only use of a stress-failure criterion is no longer sufficient. A critical deflection condition must be employed also. Application to several laminated beams made of 8 layers of diamond braided HTA (T300) carbon fabrics and R57 epoxy matrix subjected to four-point bending has been made. The predicted ultimate strengths of the laminates agree well with our experimental measurements.

I. Introduction

A GROWING interest in application of textile, specifically braided fabric, reinforced composites in several industries has been observed in recent years.[1–3] (Also see website of ICEX Socket System, URL: http://www.ossur.com/products [cited 22 April 2002].) Whereas a number of investigations have been carried out to characterize and model the elastic properties of these composites[4–9] based on their constituent properties and geometric parameters, limited investigators have analyzed the failure behaviors and ultimate strengths of braid composites subjected to in-plane loads.[10–12] So far, very few attempts have been made toward understanding the progressive failure behavior and the ultimate strength of laminated braided fabric-reinforced composites under flexural loads. Because most such composite materials in applications are more often subjected to lateral loads, knowledge of the bending properties of braided laminates is necessary for design as well as for efficient use.

In the present paper, a micromechanics-based method is applied to estimate the ultimate bending strength of laminates reinforced with multilayer braided fabric preforms. The method is a combination of the classical lamination theory and the bridging micromechanics model.[13] The lamination theory is applied to determine the load shared by each braided fabric-reinforced lamina based on the information of the lamina instantaneous compliance matrix at the previous load level. Then, the lamina analysis is carried out, by subdividing the lamina into a series of unidirectional (UD) composites in their local coordinates. The responses of the UD composites are obtained in terms of the bridging model, which are later assembled to give the lamina response including the internal stresses in the constituent fiber and matrix materials and the lamina instantaneous compliance matrix at the current load level. The maximum normal stress criterion is applied to detect the failure status of the constituent materials. If any fails, the lamina is considered to have failed, and a progressive failure strength results. However, the laminate ultimate bending strength cannot be determined only based on the stress failure criterion. This is different from the situation where the laminate is only subjected to an in-plane load. The reason is that, under a lateral load, the ultimate bending failure of the laminate generally occurs before its last-ply failure. Hence, an additional critical deflection condition also must be employed. This critical deflection is the measured deflection when the laminated beam attains its ultimate bending load.

Several laminated beams made from eight layers of diamond braided carbon fiber fabrics and an epoxy matrix, arranged in $[\theta_1/\theta_2/\theta_3/\theta_4/\theta_5/\theta_6/\theta_7/\theta_8]$, subjected to four-point bending were analyzed, where θ_1 is the top layer (facing the load) and θ_8 the bottom layer. All of the longitudinal directions (Fig. 1) of the laminas in the laminate were in accordance with the beam axial direction, with θ being the braiding angle of a specific lamina. The following laminate layups have been employed: [5/5/5/5/5/5/5/5], [15/15/15/15/15/15/15/15], [5/5/15/15/15/15/5/5], [15/15/5/5/5/5/15/15], [5/5/15/15/5/5/15/15], and [15/15/5/5/15/15/5/5]. Experiments have been carried out to measure the load-deflection curves of the beams, from which the bending stiffnesses, ultimate bending loads, and the critical deflections are obtained. These results are compared with the theoretical ones. Favorable agreement has been found.

II. Theory

The analysis is carried out layer by layer and comprises two parts: the laminate analysis, which is accomplished using the classical lamination theory, and the lamina analysis, which is based on the bridging model.

A. Laminate Analysis

A schematic diagram for a laminated braid beam, together with the definition of a global coordinate system, is shown in Fig. 1. According to the classical lamination theory,[14] the in-plane stress and strain increments of a lamina in the laminate are correlated through

Received 24 October 2000; revision received 12 September 2001; accepted for publication 24 December 2001.

*Professor, Department of Engineering Mechanics, 1239 Siping Road; huangzm@mail.tongji.edu.cn; huangzm@email.com.

†Research Scholar, Polymer and Textile Composites Laboratory, Department of Mechanical Engineering, 10 Kent Ridge Crescent.

‡Associate Professor, Polymer and Textile Composites Laboratory, Department of Mechanical Engineering, 10 Kent Ridge Crescent.

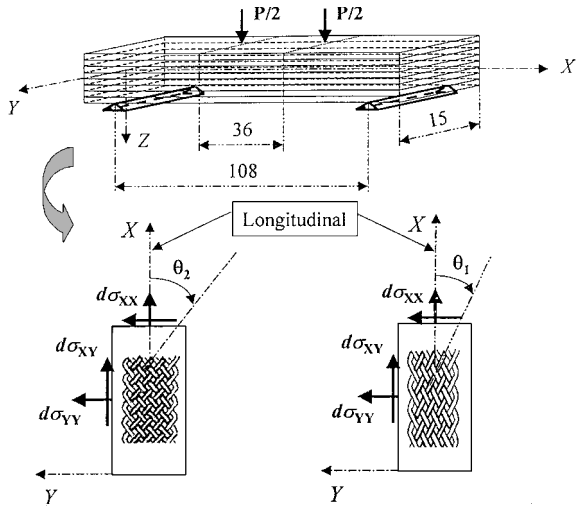

Fig. 1 Laminated beam subjected to four-point bending, with each layer being a diamond braided fabric-reinforced composite lamina.

$$\{d\sigma\}_k^G = [C]_k^G\{d\varepsilon\}_k^G = \left[\left(C_{ij}^G\right)_k\right]\{d\varepsilon\}_k^G \tag{1a}$$

$$\{d\varepsilon\}_k^G = \left\{d\varepsilon_{XX}^0 + [(Z_k + Z_{k-1})/2]d\kappa_{XX}^0, d\varepsilon_{YY}^0 + [(Z_k + Z_{k-1})/2]d\kappa_{YY}^0, 2d\varepsilon_{XY}^0 + (Z_k + Z_{k-1})d\kappa_{XY}^0\right\}^T \tag{1b}$$

where $\{d\sigma\}^G = \{d\sigma_{XX}, d\sigma_{YY}, d\sigma_{YY}\}^T$, G refers to the global system, k is the kth lamina, and T is a transposition. Z_k and Z_{k-1} are the Z coordinates of the top and bottom surfaces of the kth lamina. Here $d\varepsilon_{XX}^0$, $d\varepsilon_{YY}^0$, and $d\varepsilon_{XY}^0$ and $d\kappa_{XX}^0$, $d\kappa_{YY}^0$, and $d\kappa_{XY}^0$ are the strain and the curvature increments of the middle surface, which are determined by solving the following lamination equations[14]:

$$\begin{Bmatrix} dN_{XX} \\ dN_{YY} \\ dN_{XY} \\ dM_{XX} \\ dM_{YY} \\ dM_{XY} \end{Bmatrix} = \begin{bmatrix} Q_{11}^I & Q_{12}^I & Q_{13}^I & Q_{11}^{II} & Q_{12}^{II} & Q_{13}^{II} \\ Q_{12}^I & Q_{22}^I & Q_{23}^I & Q_{12}^{II} & Q_{22}^{II} & Q_{23}^{II} \\ Q_{13}^I & Q_{23}^I & Q_{33}^I & Q_{13}^{II} & Q_{23}^{II} & Q_{33}^{II} \\ Q_{11}^{II} & Q_{12}^{II} & Q_{13}^{II} & Q_{11}^{III} & Q_{12}^{III} & Q_{13}^{III} \\ Q_{12}^{II} & Q_{22}^{II} & Q_{23}^{II} & Q_{12}^{III} & Q_{22}^{III} & Q_{23}^{III} \\ Q_{13}^{II} & Q_{23}^{II} & Q_{33}^{II} & Q_{13}^{III} & Q_{23}^{III} & Q_{33}^{III} \end{bmatrix} \begin{Bmatrix} d\varepsilon_{XX}^0 \\ d\varepsilon_{YY}^0 \\ 2d\varepsilon_{XY}^0 \\ d\kappa_{XX}^0 \\ d\kappa_{YY}^0 \\ 2d\kappa_{XY}^0 \end{Bmatrix}$$

$$Q_{ij}^I = \sum_{k=1}^{N}\left(C_{ij}^G\right)_k(Z_k - Z_{k-1})$$

$$Q_{ij}^{II} = \frac{1}{2}\sum_{k=1}^{N}\left(C_{ij}^G\right)_k\left(Z_k^2 - Z_{k-1}^2\right)$$

$$Q_{ij}^{III} = \frac{1}{3}\sum_{k=1}^{N}\left(C_{ij}^G\right)_k\left(Z_k^3 - Z_{k-1}^3\right), \qquad h = \sum_{k=1}^{N}(Z_k - Z_{k-1}) \tag{2}$$

N is the total number of the lamina plies in the laminate. Here dN_{XX}, dN_{YY}, and dN_{XY} and dM_{XX}, dM_{YY}, and dM_{XY} are force and moment increments per unit length applied on the cross section of the laminate. When it is supposed that the beam is subjected to a simple bending with only dM_{XX} being of nonzero, the middle-plane deflection increment dw^0 can be integrated from the equation

$$\frac{\partial^2(dw^0)}{\partial X^2} = -d\kappa_{XX}^0 \tag{3}$$

with the appropriate boundary conditions. The total deflection is simply updated from $w^0 = w^0 + dw^0$.

Under the bending condition, each lamina in the laminate is subjected to essentially a different load share. Hence, some lamina must fail first before the others. Suppose that the k_0th lamina ply has failed. The remaining stiffness of the laminate must be reduced. When a total reduction strategy is used,[13] the overall stiffness elements for the next step calculation are redefined as

$$Q_{ij}^I = \sum_{\substack{k=1 \\ k\neq k_0}}^{N}\left(C_{ij}^G\right)_k(Z_k - Z_{k-1})$$

$$Q_{ij}^{II} = \frac{1}{2}\sum_{\substack{k=1 \\ k\neq k_0}}^{N}\left(C_{ij}^G\right)_k\left(Z_k^2 - Z_{k-1}^2\right)$$

$$Q_{ij}^{III} = \frac{1}{3}\sum_{\substack{k=1 \\ k\neq k_0}}^{N}\left(C_{ij}^G\right)_k\left(Z_k^3 - Z_{k-1}^3\right) \tag{4}$$

In this way, a progressive failure process can be estimated.

It must be realized that the predicted failure process (as well as load-deflection curve) may no longer be correct after the failure of an intermediate ply, which corresponds to the ultimate failure. The reason is that in reality the ultimate bending load (which is defined as the maximum load the laminate can sustain) is generally attained by the laminate before its last-ply failure. After the ultimate bending load, the load-deflection curve of the beam is downward, a phenomenon named the material softening. However, when the incremental solution strategy described earlier is used, the predicted load-deflection curve is always upward till the last-ply failure. This means that, when the laminate is involved with a lateral load, the only use of a stress failure criterion is no longer sufficient for determining its ultimate strength. An additional critical condition, which can only be the critical deflection or curvature condition, must also be employed.

B. Bridging Model

The bridging micromechanics model[13] has been developed with respect to a UD composite in its local coordinate system (x_1, x_2, x_3). Note that the x_1 axis is always along the longitudinal (fiber axial) direction.

1. *Lamina Instantaneous Compliance Matrix*

Here,

$$[S_{ij}] = \left(V_f\left[S_{ij}^f\right] + V_m\left[S_{ij}^m\right][A_{ij}]\right)(V_f[I] + V_m[A_{ij}])^{-1} = \left(V_f\left[S_{ij}^f\right] + V_m\left[S_{ij}^m\right][A_{ij}]\right)[B_{ij}] \tag{5}$$

where $[B_{ij}] = (V_f[I] + V_m[A_{ij}])^{-1}$. Note that f and m are the fiber and matrix. V_f is the fiber volume fraction, with $V_m = 1 - V_f$, and $[I]$ is a unit matrix. $[S_{ij}^f]$ and $[S_{ij}^m]$ are the instantaneous compliance matrices of the fiber and matrix materials, respectively. $[A_{ij}]$ is a bridging matrix.

2. *Bridging Matrix Elements*

The bridging matrix is given by[13]

$$[A_{ij}] = \begin{bmatrix} a_{11} & a_{12} & a_{13} & a_{14} & a_{15} & a_{16} \\ 0 & a_{22} & a_{23} & a_{24} & a_{25} & a_{26} \\ 0 & 0 & a_{33} & a_{34} & a_{35} & a_{36} \\ 0 & 0 & 0 & a_{44} & a_{45} & a_{46} \\ 0 & 0 & 0 & 0 & a_{55} & a_{56} \\ 0 & 0 & 0 & 0 & 0 & a_{66} \end{bmatrix} \tag{6a}$$

where the independent bridging elements (on the diagonal) are defined as[13]

$$a_{11} = E_m \Big/ E_{11}^f \tag{6b}$$

$$a_{22} = a_{33} = a_{44} = 0.5\left(1 + E_m \big/ E_{22}^f\right) \tag{6c}$$

$$a_{55} = a_{66} = 0.5\left(1 + G_m \big/ G_{12}^f\right) \tag{6d}$$

$$E_m = \begin{cases} E^m, & \text{when} \quad \tau_0^m \le \sqrt{2}\sigma_Y^m \big/ 3 \\ E_T^m, & \text{when} \quad \tau_0^m > \sqrt{2}\sigma_Y^m \big/ 3 \end{cases}$$

$$G_m = \begin{cases} 0.5E^m/(1+\nu^m), & \text{when} \quad \tau_0^m \le \sqrt{2}\sigma_Y^m \big/ 3 \\ E_T^m \big/ 3, & \text{when} \quad \tau_0^m > \sqrt{2}\sigma_Y^m \big/ 3 \end{cases}$$

$$\tau_0 = \left[\tfrac{1}{3}\sigma'_{ij}\sigma'_{ij}\right]^{\frac{1}{2}} = \left(1\big/\sqrt{3}\right)\left[(\sigma'_{11})^2 + (\sigma'_{22})^2 + (\sigma'_{33})^2 + 2\left\{(\sigma'_{12})^2 + (\sigma'_{13})^2 + (\sigma'_{23})^2\right\}\right]^{\frac{1}{2}}$$

$$\sigma'_{ij} = \sigma_{ij} - \tfrac{1}{3}\sigma_{kk}\delta_{ij} = \sigma_{ij} - \tfrac{1}{3}(\sigma_{11} + \sigma_{22} + \sigma_{33})\delta_{ij}$$

$$\delta_{ij} = \begin{cases} 0, & \text{if} \quad i \ne j \\ 1, & \text{if} \quad i = j \end{cases}, \qquad i, j = 1, 2, 3$$

where E, G, and ν are Young's modulus, shear modulus, and Poisson's ratio. Here σ_Y^m and E_T^m are yield strength and hardening modulus (tangent to the stress–strain curve in the plastic region) of the matrix and τ_0^m is an octahedral shear stress of the matrix. The dependent bridging elements, that is the up triangular elements in Eq. (6a), are determined by substituting Eq. (6a) into Eq. (5) and by requiring the resulting compliance matrix to be symmetric, namely,

$$S_{ij} = S_{ji}, \qquad i, j = 1, 2, \ldots, 6 \tag{7}$$

3. Internal Stresses in the Constitutents

The internal stress increments in the fiber and matrix are derived as[13]

$$\left\{d\sigma_i^f\right\} = (V_f[I] + V_m[A_{ij}])^{-1}\{d\sigma_j\} = [B_{ij}]\{d\sigma_j\} \tag{8a}$$

$$\left\{d\sigma_i^m\right\} = [A_{ij}](V_f[I] + V_m[A_{ij}])^{-1}\{d\sigma_j\} = [A_{ij}][B_{ij}]\{d\sigma_j\} \tag{8b}$$

The total stresses are updated from

$$\left\{\sigma_i^f\right\} = \left\{\sigma_i^f\right\} + \left\{d\sigma_i^f\right\}, \qquad \left\{\sigma_i^m\right\} = \left\{\sigma_i^m\right\} + \left\{d\sigma_i^m\right\}$$

$$\{\sigma_i\} = \{\sigma_i\} + \{d\sigma_i\} \tag{9}$$

where $\{d\sigma\} = \{d\sigma_{11}, d\sigma_{22}, d\sigma_{33}, d\sigma_{23}, d\sigma_{13}, d\sigma_{12}\}^T$ are the overall stress increments applied on the UD composite. The initial internal stresses in Eq. (9) assume zero values if no residual thermal stress is involved. Otherwise, a procedure provided in Ref. 15 can be employed to calculate the initial thermal residual stresses.

4. Constituent Instantaneous Compliance Matrices

The fiber material is assumed to be transversely isotropic and linearly elastic until rupture, whose instantaneous compliance matrix can be defined using Hooke's law. The matrix is considered as elastic–plastic, the instantaneous compliance matrix of which is defined using the Prandtl–Reuss theory. Detailed formulas can be found in Ref. 16, for example.

C. Failure Criteria

Both the internal stresses and the overall stresses on the lamina at the current load level are explicitly known from Eqs. (9). Thus, a failure criterion either for a UD composite or for a constituent material can be applied. However, the failure criteria for UD composites are much more inconvenient to apply. These criteria, such as the Tsai–Wu and Hashin–Rotem criteria, require the critical strength parameters measured from the composite. Because different composites only with different fiber volume fraction generally have different critical strength parameters, the fabrication and then the measurement for the critical strength parameters of the composite is very costly and time consuming. The situation can be even worse if the lamina layer is not a UD but a braid preform-reinforced composite. Although the critical strength parameters of the lamina have been measured, they may be less applicable to the composite lateral strength detection, because those parameters are obtained from in-plane load conditions. On the other hand, the critical strength parameters of the constituents are much easier to be determined under different load conditions, and no repeated tests are required. Moreover, by the use of the constituent critical strength parameters to control the lamina failure, the laminate properties can be estimated (designed) before fabrication. Thus, let us choose to apply a failure criterion to the constituent fiber and matrix materials. Namely, the lamina failure is assumed if any constituent attains its ultimate stress state.

The maximum normal stress criterion is among the best applicable to the constituent materials. With this criterion, the lamina is considered to have failed if any of the following conditions is satisfied:

$$\sigma_f^1 \ge \sigma_u^f, \qquad \sigma_f^3 \le -\sigma_{u,c}^f, \qquad \sigma_m^1 \ge \sigma_u^m, \qquad \sigma_m^3 \le -\sigma_{u,c}^m \tag{10}$$

where σ_f^1 and σ_f^3 and σ_m^1 and σ_m^3 are the first and the third principal stress of the fiber and matrix materials and where σ_u^f and $\sigma_{u,c}^f$ and σ_u^m and $\sigma_{u,c}^m$ are their tensile and compressive strengths obtained at the similar load condition as applied to the composite. They should be measured from bending tests. However, for the fiber material, its longitudinal tensile and compressive strengths can be used instead.

III. Analysis of a Braid Lamina

The three fundamental formulas of the bridging model, Eqs. (5), (8a), and (8b), are applicable only to the UD composite in its local coordinate system. To analyze the composite lamina reinforced with a more complicated fibrous structure such as a braided fabric, a subdivision of the lamina into UD composites and then an assemblage of these composites into the original lamina must be performed. For the present diamond braid lamina, the subdivision is schematically shown in Fig. 2. By definition, the braided fabric lamina is made by reinforcing a single layer of the braided fabric in the matrix.

A schematic diagram of a diamond braid is shown in Fig. 2a that is fabricated from two yarns, called fill and warp yarns, respectively, interlacing one after another. During the fabrication, interyarn gaps may exist. From Fig. 2a, one can see that the diamond fabric structure can be constructed by repeating some unit cell shown in Fig. 2b. Thus, the analysis of the braid lamina can be achieved through the analysis of the unit cell. However, the unit cell can be further divided into four subcells that are identical or symmetrical. Therefore, we only need to consider one subcell, which is called a representative volume element (RVE) for the braid lamina. When the procedure presented in Ref. 11 is followed, the RVE is subdivided in the fabric plane into subelements, as shown in Fig. 2c. Each subelement can have at most four material layers: the top matrix, the braider yarn 1, the braider yarn 2, and the bottom matrix layers. Yarns 1 and 2 can be regarded as UD composites in their respective local coordinate systems (Figs. 2e and 2f), with a fiber volume fraction given by[11]

$$V_f^Y = V_f\left[V \Big/ \left(\sum_{L=1}^{M} \bar{V}_{Y_1}^{(L)} + \sum_{L=1}^{M} \bar{V}_{Y_2}^{(L)}\right)\right] \tag{11}$$

where V is the volume of the RVE, V_f is the volume fraction of the RVE (the lamina), $\bar{V}_{Y_1}^{(L)}$ and $\bar{V}_{Y_2}^{(L)}$ are the volumes of the braider yarns 1 and 2 in the Lth subelement. Furthermore, the pure matrix layers can be also regarded as a UD composite with a zero fiber volume fraction (Fig. 2g). The bridging model summarized in Sec. II.B can be applied to these UD composites.

For the subdivision and then the definition of the yarn local coordinate systems to be achieved, the fill and warp yarn orientation in the global coordinate system must be identified. Details are given in Ref. 11. When the responses of the UD composites in their local coordinate systems have been determined, an assemblage is required to obtain the properties of the RVE, that is, the lamina. This has been given in detail in Ref. 11. Only relevant formulas are cited here.

Note that the assemblage consists of two parts: The first part is performed along the thickness direction with respect to a subelement and the second part in the lamina plane with respect to all

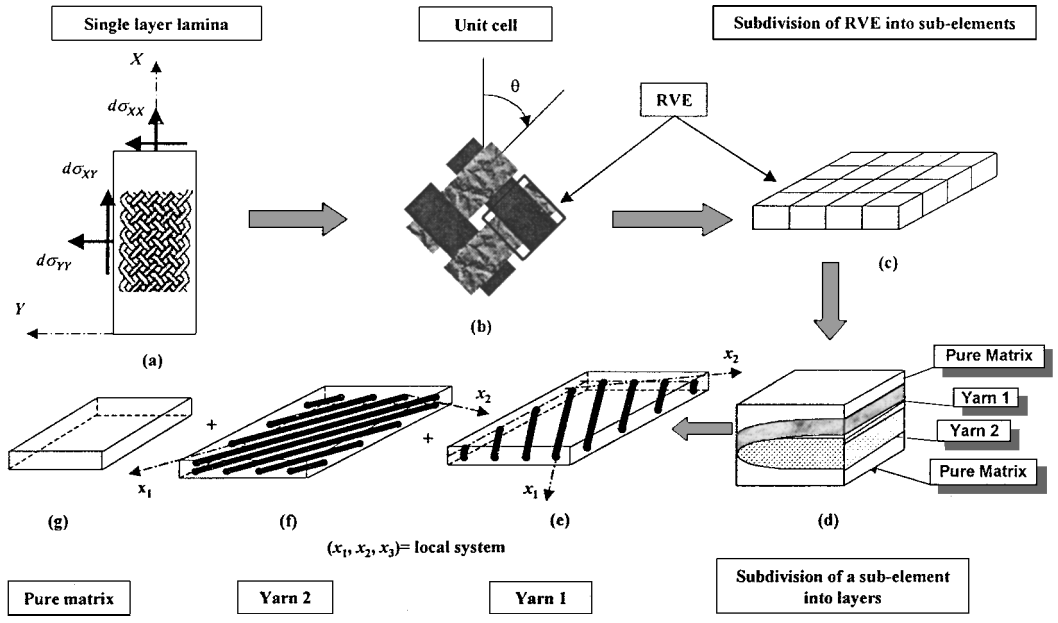

Fig. 2 Schematic diagram to show analysis procedure for a braided fabric lamina.

of the subelements. Thus, for the Lth subelement and by using an isostrain condition (which is equivalent to the classical lamination theory if bending curvatures are neglected), we have the following[11]:

$$\left[S_{ij}^{G}\right]^{(L)} = \left\{ V_{Y_1}^{(L)} \left(\left[S_{ij}^{G}\right]_{Y_1}^{(L)}\right)^{-1} + V_{Y_2}^{(L)} \left(\left[S_{ij}^{G}\right]_{Y_2}^{(L)}\right)^{-1} + \left(1 - V_{Y_1}^{(L)} - V_{Y_2}^{(L)}\right)\left(\left[S_{ij}^{m}\right]\right)^{-1} \right\}^{-1} \tag{12}$$

$$\left\{d\sigma_i^f\right\}_{Y_1}^{G,(L)} = \left([T_{ij}]_c\right)_{Y_1}^{(L)} [B_{ij}] \left([T_{ij}]_s^T\right)_{Y_1}^{(L)} \left[C_{ij}^{G}\right]_{Y_1}^{(L)} \left[S_{ij}^{G}\right]^{(L)} \{d\sigma_j\}^{G,(L)} \tag{13a}$$

$$\left\{d\sigma_i^f\right\}_{Y_2}^{G,(L)} = \left([T_{ij}]_c\right)_{Y_2}^{(L)} [B_{ij}] \left([T_{ij}]_s^T\right)_{Y_2}^{(L)} \left[C_{ij}^{G}\right]_{Y_2}^{(L)} \left[S_{ij}^{G}\right]^{(L)} \{d\sigma_j\}^{G,(L)} \tag{13b}$$

$$\left\{d\sigma_i^m\right\}^{G,(L)} = V_{Y_1}^{(L)} \left\{d\sigma_i^m\right\}_{Y_1}^{G,(L)} + V_{Y_2}^{(L)} \left\{d\sigma_i^m\right\}_{Y_2}^{G,(L)} + \left(1 - V_{Y_1}^{(L)} - V_{Y_2}^{(L)}\right) \left\{d\sigma_i^m\right\}_{m}^{G,(L)} \tag{13c}$$

$$\left\{d\sigma_i^m\right\}_{Y_1}^{G,(L)} = \left([T_{ij}]_c\right)_{Y_1}^{(L)} [A_{ij}][B_{ij}] \left([T_{ij}]_s^T\right)_{Y_1}^{(L)} \left[C_{ij}^{G}\right]_{Y_1}^{(L)} \left[S_{ij}^{G}\right]^{(L)} \{d\sigma_j\}^{G,(L)} \tag{14a}$$

$$\left\{d\sigma_i^m\right\}_{Y_2}^{G,(L)} = \left([T_{ij}]_c\right)_{Y_2}^{(L)} [A_{ij}][B_{ij}] \left([T_{ij}]_s^T\right)_{Y_2}^{(L)} \left[C_{ij}^{G}\right]_{Y_2}^{(L)} \left[S_{ij}^{G}\right]^{(L)} \{d\sigma_j\}^{G,(L)} \tag{14b}$$

$$\left\{d\sigma_i^m\right\}_{m}^{G,(L)} = \left(\left[S_{ij}^{m}\right]\right)^{-1} \left[S_{ij}^{G}\right]^{(L)} \{d\sigma_j\}^{G,(L)} \tag{14c}$$

In the preceding equations, G designates that the relevant quantity is expressed in the global coordinate system. L is the current Lth subelement. Thus, $\{d\sigma\}^{G,(L)} = (\{d\sigma_{XX}, d\sigma_{YY}, d\sigma_{ZZ}, d\sigma_{YZ}, d\sigma_{XZ}, d\sigma_{XY}\}^{(L)})^T \equiv (\{d\sigma_{XX}, d\sigma_{YY}, 0, 0, 0, d\sigma_{XY}\}^{(L)})^T$. It must be realized that the plane stress increments, obtained from Eq. (1a), should be extended into a three-dimensional form. $V_{Y_1}^{(L)} = \bar{V}_{Y_1}^{(L)} / \bar{V}^{(L)}$ and $V_{Y_2}^{(L)} = \bar{V}_{Y_2}^{(L)} / \bar{V}^{(L)}$, where $\bar{V}^{(L)}$ is the volume of the subelement. The yarn global compliance and stiffness matrices are calculated from

$$\left[S_{ij}^{G}\right]_{Y}^{(L)} = \left([T_{ij}]_s\right)_{Y}^{(L)} [S_{ij}] \left([T_{ij}]_s^T\right)_{Y}^{(L)}, \qquad Y = Y_1 \text{ and } Y_2 \tag{15a}$$

$$\left[C_{ij}^{G}\right]_{Y}^{(L)} = \left(\left[S_{ij}^{G}\right]_{Y}^{(L)}\right)^{-1} \tag{15b}$$

Refer to Ref. 11 for the coordinate transformation matrices $\left([T_{ij}]_s\right)_{Y}^{(L)}$ and $\left([T_{ij}]_c\right)_{Y}^{(L)}$. By use of an isostress condition,[11] the overall instantaneous compliance matrix of the RVE is given by

$$\left[S_{ij}^{G}\right] = \frac{1}{V} \sum_{L=1}^{M} \bar{V}^{(L)} \left[S_{ij}^{G}\right]^{(L)} \tag{16}$$

The averaged stress increments in the fibers and the matrix are obtained from

$$\left\{d\sigma_i^f\right\}^{G} = \frac{1}{2V} \sum_{L=1}^{M} \bar{V}^{(L)} \left(\left\{d\sigma_i^f\right\}_{Y_1}^{G,(L)} + \left\{d\sigma_i^f\right\}_{Y_2}^{G,(L)} \right)$$

$$= \frac{1}{2V} \left(\sum_{L=1}^{M} \bar{V}^{(L)} \left\{ \left([T_{ij}]_c\right)_{Y_1}^{(L)} [B_{ij}] \left([T_{ij}]_s^T\right)_{Y_1}^{(L)} \left[C_{ij}^{G}\right]_{Y_1}^{(L)} + \left([T_{ij}]_c\right)_{Y_2}^{(L)} [B_{ij}] \left([T_{ij}]_s^T\right)_{Y_2}^{(L)} \left[C_{ij}^{G}\right]_{Y_2}^{(L)} \right\} \left[S_{ij}^{G}\right]^{(L)} \right) \{d\sigma_j\}^{G} \tag{17a}$$

$$\left\{d\sigma_i^m\right\}^{G} = \frac{1}{V} \sum_{L=1}^{M} \bar{V}^{(L)} \left\{d\sigma_i^m\right\}^{G,(L)} \tag{17b}$$

$$\left\{d\sigma_i^m\right\}^{G,(L)} = \left\langle V_{Y_1}^{(L)} \left([T_{ij}]_c\right)_{Y_1}^{(L)} [A_{ij}][B_{ij}] \left([T_{ij}]_s^T\right)_{Y_1}^{(L)} \left[C_{ij}^{G}\right]_{Y_1}^{(L)} + V_{Y_2}^{(L)} \left([T_{ij}]_c\right)_{Y_2}^{(L)} [A_{ij}][B_{ij}] \left([T_{ij}]_s^T\right)_{Y_2}^{(L)} \left[C_{ij}^{G}\right]_{Y_2}^{(L)} + \left(1 - V_{Y_1}^{(L)} - V_{Y_2}^{(L)}\right) \left[S_{ij}^{m}\right]^{-1} \right\rangle \left[S_{ij}^{G}\right]^{(L)} \{d\sigma_j\}^{G} \tag{17c}$$

Finally, the full three-dimensional compliance matrix [Eq. (16)] must be adapted for the next incremental step laminate analysis. This is done as follows:

$$\left[C_{ij}^{G}\right] = \begin{bmatrix} C_{11}^{G} & C_{12}^{G} & C_{13}^{G} \\ & C_{22}^{G} & C_{23}^{G} \\ \text{symmetric} & & C_{33}^{G} \end{bmatrix} = \begin{bmatrix} S_{11}^{G} & S_{12}^{G} & S_{16}^{G} \\ & S_{22}^{G} & S_{26}^{G} \\ \text{symmetric} & & S_{66}^{G} \end{bmatrix}^{-1}$$

IV. Results and Discussion

Experiments have been performed to fabricate an epoxy matrix-based composite laminate with eight layers of diamond braided fabric reinforcement. The flat fabrics of 5- and 15-deg braiding angles were prepared using HTA carbon fibers (diameter of 7 μm, 6000 filaments; TOHO Rayon Co., Ltd., Japan), which are comparable in properties to T300 carbon fibers. The matrix was a mixture of resin R57 and hardener H3057 (Chemicrete Co., Singapore) in a weight ratio of 100 (resin):60 (hardener). Six lamination arrangements were used: $[5\ \text{deg}]_8$, $[15\ \text{deg}]_8$, [5/5/15/15/15/15/5/5], [15/15/5/5/5/5/15/15], [15/15/5/5/15/15/5/5], and [5/5/15/15/5/5/15/15]. The resin-impregnated fabrics were laid in the female part of a mold, followed by a pressure connection with the male part, and were cured at room temperature. The composite beam resulted after the removal of the mold, having a width of 15 mm. The fabric geometric parameters as fabricated, including the yarn width and thickness and interyarn gaps, were accurately measured before resin impregnation. These parameters are necessary to specify the yarn orientation in the fabric.[11] The laminate overall fiber volume fraction was measured using a combustion method and is, together with the laminate thickness, given in Table 1. For simplicity, each lamina in the laminate was assumed to have the same thickness. However, for those laminates that have both 5- and 15-deg braiding angle fabrics as reinforcement, the fiber volume fraction in each layer was determined by a multiplication of a thickness ratio with the fiber volume fraction of the corresponding laminate reinforced with their respective fabrics alone. For instance, the [5/5/5/5/5/5/5/5] beam had a fiber volume fraction of 0.555, and the thickness of each layer in this laminate was 0.569 mm. On the other hand, the thickness of each lamina layer in the [5/5/15/15/15/15/5/5] laminate was 0.599 mm. Hence, the fiber volume fraction of the 5-deg braiding angle lamina in the [5/5/15/15/15/15/5/5] laminate was set to $0.527 = 0.569 \times 0.555/0.599$. The lamina fiber volume fractions thus obtained are listed in Table 1.

The laminated beams were subjected to a four-point bending test up to failure using an Instron machine (mode 4502) at a cross-head speed of 3 mm/min. The beam span, as indicated in Fig. 1, was determined following American Society for Testing and Materials D 6272. For each laminate arrangement, at least three specimens were tested. From measured load-deflection curves at one loading point, the bending stiffnesses, ultimate bending loads, and the critical deflections were obtained, where the critical deflection is the deflection of the loading point when the ultimate bending load is attained. The averaged results together with standard deviations are summarized in Table 1. It is seen that the deviations are acceptably small.

Before the theoretical modeling, the constituent properties must be specified. The fiber (T300) elastic parameters were taken from Ref. 17 and are summarized in Table 2. The fiber tensile and compressive strengths, $\sigma_u^f = 2467.8$ MPa and $\sigma_{u,c}^f = 1470.4$ MPa, were retrieved using the formulas given in Ref. 18 on the longitudinal tensile and compressive strengths of a UD composite made from the T300 fibers and an epoxy resin.[17] These results are also listed in Table 2. The R57 matrix elastic–plastic properties were experimentally determined using monolithic specimens subjected to four-point bending. Strain gauges were employed to measure both the tensile (the top surface) and the compressive (the bottom surface) responses of the matrix specimens. The matrix parameters thus obtained are summarized in Table 3. It is noted that matrix Poisson's ratio and compressive strength were measured from uniaxial compression tests.

When the independent constituent properties and the fabric geometric parameters were used, prediction of the load-deflection responses of the six braided fabric composite beams under four-point bending was made. The beam stiffness was calculated before the first-ply failure. Then, the load level and the corresponding deflection of a loading point at each-ply failure were estimated, which are called, respectively, the ply-failure load and the ply-failure deflection for the convenience of expression. Results are summarized in Table 4. When a calculated ply-failure deflection is closest to the measured critical deflection, the corresponding ply-failure load is defined as the ultimate bending load. It is seen from Table 4 that the ultimate bending load of a different laminated beam may be obtained at a different ply-failure load. The [15/15/15/15/15/15/15/15] and [15/15/5/5/5/5/15/15] laminates sustained their ultimate bending loads at the first-ply failure, whereas the [15/15/5/5/15/15/5/5] laminate attained its ultimate bending load at the second-ply failure. The remaining laminates obtained their ultimate bending loads when the third-ply failure occurred. The present predictions, both in bending stiffness and in ultimate bending load, agree well with the experiments, indicating that the bridging model combined with the classical lamination theory is efficient for the failure analysis and strength prediction of laminated beams under flexural loads.

Table 2 Properties of T300 carbon fibers

Property	Value
E_{11}^f, GPa	230
E_{22}^f, GPa	15
ν_{12}^f	0.2
G_{12}^f, GPa	15
ν_{23}^f	0.07
σ_u^f, MPa	2467.8
$\sigma_{u,c}^f$, MPa	1470.4

Table 1 Measured properties of laminated braid T300/R57 beams

			Lamina parameters		Bending stiffness, N/mm	Ultimate load, N	Critical displacement,[e] mm
Layup	H_B,[a] mm	V_f[b]	θ,[c] deg	V_f[d]	(standard deviation)	(standard deviation)	(standard deviation)
$[5]_8$	4.55	0.555	5	0.555	681.0 (3.4)	3005.3 (13.1)	4.423 (0.42)
$[15]_8$	4.63	0.560	15	0.560	626.6 (1.2)	2463.7 (7.9)	4.114 (0.24)
[5/5/15/15/15/15/5/5]	4.79	0.534	5	0.527	759.1 (7.1)	3237.9 (9.8)	4.294 (0.38)
			15	0.541			
[15/15/5/5/5/5/15/15]	4.62	0.554	5	0.547	595.4 (9.6)	2322.0 (21.3)	4.100 (0.51)
			15	0.561			
[15/15/5/5/15/15/5/5]	4.68	0.547	5	0.54	659.3 (6.2)	2896.7 (10.3)	4.508 (0.35)
			15	0.554			
[5/5/15/15/5/5/15/15]	4.73	0.542	5	0.534	667.4 (2.5)	2972.8 (14.2)	4.640 (0.33)
			15	0.549			

[a]Beam thickness. [b]Overall fiber volume fraction of the beam. [c]Braiding angle. [d]Fiber volume fraction of the lamina.
[e]Deflection corresponding to ultimate load.

Table 3 Bending properties of R57 epoxy matrix ($\nu^m = 0.414$)

	Tensile behavior						Compressive behavior		
Property[a]	1	2	3	4	5	6	1	2	3
$(\sigma_Y^m)_i$, MPa	21.2	36.6	50.6	59.2	69.0	78.9[b]	40.2	63.7	83.5[b]
$(E_T^m)_i$, GPa	2.93	2.62	2.32	1.75	1.32	0.56	3.09	2.76	1.32

[a]$E_m = (E_T^m)_i$, when $(\sigma_Y^m)_{i-1} \le \sigma_e^m \le (\sigma_Y^m)_i$, with $(\sigma_Y^m)_0 = 0$.
[b]Ultimate strength value.

Table 4 Predicted properties of laminated braid beams under four-point bending

	First-ply failure		Second-ply failure		Third-ply failure		Bending	Ultimate
Layup	Load, N	Displacement, mm	Load, N	Displacement, mm	Load, N	Displacement, mm	stiffness, N/mm (relative error, %)	load, N (relative error, %)
[5/5/5/5/5/5/5/5]	2314.6	3.236	2761.5	3.859	3185.4	4.448	715.0 (5.0)	3185.4 (6.0)
[15/15/15/15/15/15/15/15]	2303.2	4.349	2738.5	5.168	3162.5	5.962	529.5 (15.5)	2303.2 (6.5)
[5/5/15/15/15/15/5/5]	2360.4	3.099	2784.3	3.653	3334.3	4.371	761.5 (0.4)	3334.3 (3.0)
[15/15/5/5/5/5/15/15]	2406.3	4.326	2899.0	5.209	3002.1	5.393	556.2 (6.6)	2406.3 (3.6)
[15/15/5/5/15/15/5/5]	2624.0	4.042	3151.0	4.847	3242.7	4.987	648.9 (1.6)	3151.0 (8.8)
[5/5/15/15/5/5/15/15]	2165.7	3.257	2578.2	3.877	3254.2	4.889	664.9 (0.4)	3254.2 (9.5)
Averaged error, %							4.9	6.2

V. Conclusions

A theoretical method combining the classical lamination theory and the bridging micromechanics model has been presented to simulate the progressive failure strengths of a laminated composite made using braided fabric reinforcement until the ultimate failure takes place (the ultimate bending strength occurs). The method has been verified using the experimental data of six braided fabric-reinforced composite laminates subjected to four-point bending. It has been shown that the ultimate bending strength of a laminated composite generally does not correspond to its last-ply failure stress level. An additional critical deflection condition is also required to determine the laminate ultimate strength when a lateral load is involved. The present method is not applicable to the prediction of a laminate response after the ultimate bending strength has been attained.

References

[1]Kostar, T. D., and Chou, T. W., "Braided Structures," *3-D Textile Reinforcements in Composite Materials*, edited by A. Miravete, Woodhead, Cambridge, England, U.K., 1999, pp. 217–238.

[2]Fujihara, K., Huang, Z. M., Ramakrishna, S., Satkunanantham, K., and Hamada, H., "Development of Braided Carbon/PEEK Composite Bone Plates," *Advanced Composites Letters*, Vol. 10, No. 1, 2001, pp. 13–20.

[3]Thomson, D., "Braiding Applications for Civil Infrastructure," *SAMPE Journal*, Vol. 35, No. 4, 1999, pp. 38–41.

[4]Yang, J. M., Ma, C. L., and Chou, T. W., "Fiber Inclination Model of Three Dimensional Textile Structural Composites," *Journal of Composite Materials*, Vol. 20, 1986, pp. 472–484.

[5]Byun, J. H., Whitney, T. J., Du, G. W., and Chou, T. W., "Analytical Characterization of Two-Step Braided Composites," *Journal of Composite Materials*, Vol. 25, 1991, pp. 1599–1618.

[6]Masters, J. E., Foye, R. L., Pastore, C. M., and Gowayed, Y. A., "Mechanical Properties of Triaxially Braided Composites: Experimental and Analytical Results," *Journal of Composite Technology and Research*, Vol. 15, 1993, pp. 112–122.

[7]Dadkhah, M. S., Flintoff, J. G., Kniveton, T., and Cox, B. N., "Simple-Models for Triaxially Braided Composites," *Composites*, Vol. 26, No. 8, 1995, pp. 561–577.

[8]Bogdanovich, A. E., and Pastore, C. M., "Material-Smart Analysis of Textile-Reinforced Structures," *Composite Science and Technology*, Vol. 56, No. 3, 1996, pp. 291–309.

[9]Chen, L., Tao, X. M., and Choy, C. L., "Mechanical Analysis of 3-D Braided Composites by the Finite Multiphase Element Method," *Composite Science and Technology*, Vol. 59, No. 16, 1999, pp. 2383–2391.

[10]Naik, R. A., "Failure Analysis of Woven and Braided Fabric Reinforced Composites," *Journal of Composite Materials*, Vol. 29, 1995, pp. 2334–2363.

[11]Huang, Z. M., "The Mechanical Properties of Composites Reinforced with Woven and Braided Fabrics," *Composite Science and Technology*, Vol. 60, 2000, pp. 479–498.

[12]Harte, A. M., and Fleck, N. A., "Deformation and Failure Mechanisms of Braided Composite Tubes in Compression and Torsion," *Acta Materialia*, Vol. 48, No. 6, 2000, pp. 1259–1271.

[13]Huang, Z. M., "Simulation of the Mechanical Properties of Fibrous Composites by the Bridging Micromechanics Model," *Composites Part A*, Vol. 32, No. 2, 2001, pp. 143–172.

[14]Gibson, R. F., *Principles of Composite Material Mechanics*, McGraw–Hill, New York, 1994.

[15]Huang, Z. M., "Modeling Strength of Multidirectional Laminates Under Thermo-Mechanical Loads," *Journal of Composite Materials*, Vol. 35, No. 4, 2001, pp. 281–315.

[16]Huang, Z. M., "Tensile Strength of Fibrous Composites at Elevated Temperature," *Material Science and Technology*, Vol. 16, 2000, pp. 81–94.

[17]Soden, P. D., Hinton, M. J., and Kaddour, A. S., "Lamina Properties, Lay-Up Configurations and Loading Conditions for a Range of Fiber-Reinforced Composite Laminates," *Composite Science and Technology*, Vol. 58, 1998, pp. 1011–1022.

[18]Huang, Z. M., "Micromechanical Strength Formulae of Unidirectional Composites," *Materials Letters*, Vol. 40, 1999, pp. 164–169.

A. M. Waas
Associate Editor